NOTICE: this is the author's version of a work that was accepted for publication in Tunnelling and Underground Space Technology. Changes resulting from the publishing process, such as peer review, editing, corrections, structural formatting, and other quality control mechanisms may not be reflected in this document. Changes may have been made to this work since it was submitted for publication. A definitive version was subsequently published in TUNNELLING AND UNDERGROUND SPACE TECHNOLOGY 32, 158-167, (2012), DOI: 10.1016/j.tust.2012.06.007

Steady-state groundwater inflow into a circular tunnel

Christoph Butscher

Massachusetts Institute of Technology, Department of Civil and Environmental Engineering, 77 Massachusetts Avenue, Cambridge, MA 02139, USA
Corresponding author: Christoph Butscher, e-mail: butscher@mit.edu, phone: +1 617 715 4766, fax: +1 617 253 6044

Abstract

The prediction of groundwater inflow into a tunnel is important for designing the tunnel drainage system and to minimize environmental impacts and the risk of tunnel instabilities and subsidence damage. Analytical solutions exist to calculate tunnel inflow, and, increasingly, numerical groundwater models are used to this end. In order to represent different types of tunnel support structures, this study reviews different boundary conditions that can be set at the tunnel perimeter to calculate tunnel inflow and recognizes different ways to account for the tunnel lining. Analytical solutions and numerical models to calculate tunnel inflow are compared and factors influencing the accuracy of numerical solutions are highlighted. The study suggests that numerical models provide estimates of tunnel inflows with sufficient accuracy for practical purposes if the tunnel is lined and has no drainage layer surrounding the lining, and if the hydraulic conductivity of the lining is several orders of magnitude lower than the hydraulic conductivity of the aquifer, or if the lining is thick. Otherwise, the extent of the model domain must be large with respect to the extent of the tunnel to provide accurate results. It was shown that inflows are higher for lined tunnels with a drainage layer than for unlined tunnels, if the head in the drainage layer corresponds to the level of the tunnel center or invert. If the head in the drainage layer corresponds to the level of the tunnel crown, inflows are higher for unlined tunnels. The study further suggests that for unlined tunnels, inflows are higher at the invert than at the crown. For lined tunnels with a drainage layer, the reverse is true. Differences between inflows at the crown and invert decrease with increasing depth of the tunnel under the groundwater table. The numerical solution for flow into lined tunnels without drainage layer using a transfer (Cauchy type, or 3rd-kind) boundary condition produces lower inflows compared to using a specified head (Dirichlet type, or 1st-kind) boundary condition. Using a transfer boundary condition is especially inaccurate if the lining is thick.

Keywords: Tunnel inflow; Boundary conditions; Tunnel lining; Drainage; Groundwater modeling.

1. Introduction

The prediction of groundwater inflow into a tunnel is an important issue in tunnel engineering. Groundwater inflow into a tunnel can lead to problems during construction; also groundwater drawdown due to the drainage effect of the tunnel can cause surface subsidence and have other environmental impacts. Engineers need estimates of tunnel groundwater inflow for the design of the tunnel drainage systems. Several authors presented analytical solutions to calculate steady-state inflow into a circular tunnel (e.g., Lei, 1999; El Tani, 2003; Kolymbas and Wagner, 2007; Park et al., 2008). Closed form solutions have also been used successfully to account for different situations. El Tani (2010), for example, used a modified Helmholtz equation to consider a semi-infinite aquifer drained by a circular tunnel in different heterogeneous aquifer settings. In addition, efforts have been made to account for the transient nature of tunnel inflow. Maréchal and Perrochet (2003) used the analytical solution of Jacob and Lohman (1952) for artesian wells to model aquifer drainage by a tunnel. Perrochet (2005a), Perrochet and Dematteis (2007) and Yang and Yeh (2007) introduced transient solutions for calculating drilling speed-dependent discharge rates into tunnels gradually excavated in homogeneous and heterogeneous aquifers, and Perrochet (2005b) developed a simple analytical formula to calculate transient discharge inflow rates into tunnels or wells under constant drawdown. Other authors focused on analytical solutions to calculate pore water pressures in order to estimate the effective stress distribution at the tunnel perimeter (e.g., Fernández and Alvarez, 1994). However, analytical solutions to calculate tunnel inflow are only applicable in rather simple situations. To represent more complex geological situations at an actual site in a flexible way, numerical approaches that can account for spatially distributed hydraulic properties and boundary conditions (BC) are necessary. The advance of computational performance of computers led to a strong increase in the use of numerical groundwater models in tunnel engineering. Many numerical groundwater models use finite element techniques (e.g., Bear, 1972). Such models can not only account for complex geometrical situations, it is also possible to calculate the spatial distribution of the hydraulic head field, and to calculate the spatial distribution of the tunnel inflow. This is relevant for applications that require making a distinction between inflow at the tunnel crown and at the invert (e.g., Butscher et al., 2011a). In addition, numerical models can effectively be applied to transient conditions (e.g., Font-Capo et al., 2011).

Another advantage of numerical groundwater models is that they can account for a tunnel lining, which can have different hydraulic properties. Analytical solutions do either not consider a tunnel lining, or they assume inflow into a drainage layer surrounding the (impermeable) tunnel lining. In the latter case, the actual drainage of the tunnel is independent of the lining. In such a case, inflow can be represented without discretizing the lining and the drainage layer in numerical groundwater models. In cases without a drainage layer, however, one has to account for the hydraulic properties of the tunnel lining. The lining can be spatially discretized and associated with hydraulic properties (i.e., discrete elements of the finite element mesh that match the position and geometry of the lining are associated with hydraulic properties of the lining). Alternatively, the lining is not spatially discretized but a transfer rate is assigned at the tunnel perimeter representing a resistance to flow and limiting tunnel inflow.

There are many studies in the literature calculating tunnel inflow under different hydraulic conditions at the tunnel. The hydraulic conditions at the tunnel, however, have not been compiled with regard to their impact on tunnel inflows so far. In this paper, we first summarize the different ways how BC can be set at the tunnel perimeter to represent different types of tunnel support structures. We introduce existing analytical solutions and numerical models to calculate tunnel inflow, and compare the analytical solutions with numerical solutions. This comparison highlights the extent of the model domain as a constraint that limits the accuracy of numerical solutions.

Subsequently, the influence of the tunnel type on tunnel inflow is analyzed using different BC at the tunnel perimeter and different representations of the tunnel lining. The choice of the BC has an impact on total tunnel inflow and the spatial distribution of the inflow. The way in which the tunnel lining is represented can impact the accuracy of inflow calculations, especially when the lining is thick.

2. Boundary conditions at the tunnel perimeter

The type of a tunnel influences tunnel inflow and the drainage effect of the tunnel in an aquifer. A tunnel can have 1) a drainage layer surrounding the tunnel lining; 2) no such layer; or 3) can be unlined. In this chapter, we will review different types of tunnel support structures. We will show how different BC at the tunnel perimeter can be used in tunnel inflow calculations to account for the hydraulic differences as a consequence of different tunnel types. We distinguish three different types of tunnel support structures. These types, the corresponding BC at the tunnel perimeter and the way how the lining is represented are summarized in Table 1.

[Table 1 near here]

Type I represents an open tunnel without lining. The hydraulic (total) head at the tunnel perimeter corresponds to the elevation (El Tani, 2003), i.e. the hydraulic head is not uniform but higher at the tunnel crown than at the invert. This BC is based on the assumption that atmospheric pressure (zero water pressure) is effective inside the tunnel and at the tunnel perimeter. In the following, we will call this BC "elevation head BC" and the calculated tunnel inflow using this BC is referred to as "*Q1*". In numerical groundwater models, a 1st-kind BC (Dirichlet type) is set at this boundary, which involves specifying a constant value of the hydraulic head (for a given time) at the tunnel perimeter.

Type II represents a tunnel where the tunnel opening is surrounded by an impermeable lining and a drainage layer behind the lining. The hydraulic head at the tunnel perimeter (within the drainage layer) is uniform (Kolymbas and Wagner, 2007). It corresponds to the elevation of the outlet of the drainage layer, which may be adjustable (Figure 1). In the following, we will call this BC "uniform head BC" and the calculated tunnel inflow using this BC is referred to as "*Q2*". When using the uniform head BC to calculate inflow into a tunnel with drainage layer, it is assumed that the drainage layer provides no resistance to flow. This assumption is justified if the hydraulic conductivity within the drainage layer is very high compared to the hydraulic conductivity of the lining and the aquifer. Typical drainage systems today consist of geotextiles combined with geomembranes or, occasionally, pea-gravel, both with conductivities in the order of 1E-3 m/s or greater. These conductivities are very high compared to the conductivity of the lining, and higher than aquifer conductivity in most settings. In numerical groundwater models, a 1st-kind BC (specified head, Dirichlet type) is set at the tunnel perimeter, and a discretization of the drainage layer and the lining is not necessary.

[Figure 1 near here]

Type III represents a lined tunnel without drainage layer. Because of the lack of the drainage layer, the hydraulic head at the tunnel perimeter corresponds to the elevation (zero water pressure inside the tunnel). Accordingly, an elevation head BC is set at the tunnel perimeter (c.f., type I). In numerical groundwater models, there are two different ways to represent the tunnel lining: (1) A 1^{st}-kind BC (specified head, Dirichlet type) is used at the tunnel perimeter. The lining of the tunnel is spatially discretized and surrounds this boundary. The hydraulic properties of the lining are defined by its hydraulic conductivity k_l and thickness d. In Table 1, this case is referred to as tunnel type IIIa. (2) A 3^{rd}-kind BC (transfer, Cauchy type) is used at the tunnel perimeter. This BC involves specifying both a constant head and hydraulic gradient (for a given time) at the boundary. The hydraulic gradient can be specified in terms of a flow rate in numerical models, because the hydraulic conductivity will also be specified. When using a 3^{rd}-kind BC to calculate tunnel inflow, the tunnel lining is not discretized but represented by an "outflow transfer rate" at this boundary that limits flow. In Table 1, this case is referred to as tunnel type IIIb.

The 3^{rd}-kind BC is most often used to model surface water – groundwater interaction (Diersch, 2009): the exchange between a river and the groundwater, for example, depends on the river stage and the groundwater head, but is limited by a "colmation layer", leading to a certain "resistance" to flow. Recently, some authors used this type of BC also in simulating the resistance against water inflow into a tunnel provided by the tunnel lining (e.g., Font-Capo et al, 2011; Butscher et al., 2011b). The use of a 3^{rd}-kind BC at the tunnel perimeter without discretizing the lining is especially useful if the thickness of the lining is very small compared to the overall model dimension, because the thickness of the lining is typically smaller than the elements of the finite element mesh in such a case.

3. Existing analytical solutions

Simple closed-form analytical solutions to calculate steady-state inflow into a tunnel have been established for a circular tunnel in a semi-infinite aquifer. This situation is illustrated in Figure 2. Park et al. (2008) revised and compared existing analytical solutions (El Tani, 2003; Kolymbas and Wagner, 2007; Lei, 1999) and focused on solutions that either consider an unlined tunnel (type I) using an elevation head BC at the tunnel perimeter or a lined tunnel with drainage layer (type II) using a uniform head BC. They re-derived the solutions using a common notation and reference datum for the hydraulic head to make the solutions comparable. In the following, two analytical solutions (one for tunnels type I, the other for type II) are described, using the form presented by Park et al. (2008).

[Figure 2 near here]

El Tani (2003) presented an analytical solution to calculate groundwater inflow *Q1* (volume of water per unit tunnel length) into an unlined tunnel (type I) in the situation illustrated in Figure 2, considering an elevation head BC at the tunnel perimeter:

$$Q_1 = \frac{2\pi\, k_{aq}(A+H)}{ln\left(\frac{h}{r}+\sqrt{\frac{h^2}{r^2}-1}\right)} \qquad (1)$$

NOTICE: this is the author's version of a work that was accepted for publication in Tunnelling and Underground Space Technology. Changes resulting from the publishing process, such as peer review, editing, corrections, structural formatting, and other quality control mechanisms may not be reflected in this document. Changes may have been made to this work since it was submitted for publication. A definitive version was subsequently published in TUNNELLING AND UNDERGROUND SPACE TECHNOLOGY 32, 158-167, (2012), DOI: 10.1016/j.tust.2012.06.007

where $A = h(1-\alpha^2)/(1+\alpha^2)$ and (2)

$$\alpha = \frac{1}{r}\left(h - \sqrt{h^2 - r^2}\right). \quad (3)$$

The variables needed to calculate *Q1* are the hydraulic conductivity of the aquifer (k_{aq}), the hydraulic head at the top of the aquifer (*H*), the depth of the tunnel (*h*) and the tunnel radius (*r*). The geometrical parameters relate to a reference datum (c.f., Figure 2). The variables are also summarized in Table 2.

Kolymbas and Wagner (2007) presented an analytical solution to calculate tunnel inflow *Q2* into the drainage layer of lined tunnels (type-II tunnels) in the situation illustrated in Figure 2, considering a uniform head BC at the tunnel perimeter:

$$Q_2 = \frac{2\pi\, k_{aq}(-h_a + H)}{ln\left(\frac{h}{r} + \sqrt{\frac{h^2}{r^2} - 1}\right)} \quad (4)$$

In addition to the variables needed to calculate *Q1*, the uniform hydraulic head at the tunnel perimeter h_a (c.f., Figure 1) must be specified.

When we later compare tunnel inflows calculated with numerical groundwater models to analytical solutions, we refer to the solutions introduced here. If not stated differently in the text, we always use the parameters noted in Table 2 to calculate tunnel inflow.

[Table 2 near here]

4. Numerical models

We used the finite element code FEFLOW (Diersch, 2009) to simulate steady-state groundwater flow into a tunnel. The finite element representation of the situation for which the analytical solutions have been derived (c.f., Figure 2) is illustrated in Figure 3. A tunnel with radius *r* is situated in an isotropic aquifer with a hydraulic conductivity k_{aq} at depth *h* under the upper model boundary. Some models include a discretized lining around the tunnel (type IIIa) with an isotropic hydraulic conductivity k_l and thickness *d*. The lateral and downward extent of the model domain is given by *ME* (model extent). In Figure 3, the depth of the tunnel *h* corresponds to the extent of the model *ME*. However, this special situation does not apply to all models. The geometrical difference between *ME* and *h* is illustrated in Figure 4. In model 1 of this figure, *ME* equals *h* (the geometry of model 1 corresponds to the geometry of the model shown in Figure 3). In model 2 of this figure, *ME* is greater than *h*.

[Figures 3 and 4 near here]

If not stated differently, all outer model boundaries are assigned a 1st-kind (specified head, Dirichlet type) BC. The upper model boundary is the elevation reference datum with a hydraulic head $\Phi = h + H$. The groundwater level above the tunnel can be varied by varying the head assigned to this boundary. Tunnel inflow can lead to drawdown of the groundwater table if groundwater recharge is less than inflow into the tunnel. By specifying a constant hydraulic head at this boundary, drawdown of the groundwater table as a result of tunnel inflow is balanced by groundwater recharge in the models. The hydraulic head at all other outer model boundaries corresponds to the hydraulic head at the upper model boundary in most simulations, representing hydrostatic pressure conditions. Some simulations assume no-flow conditions at these boundaries.

The inner model boundary is located at the tunnel perimeter. The different types of tunnel support structures have different BC at this boundary and different implementations of the lining (c.f., Table 1). In models representing tunnels tunnel types I, II and IIIa, a 1st-kind BC is set at this boundary. The head is either variable and corresponds to the elevation (elevation head BC to calculate *Q1*; types I and III), i.e., the head is higher at the crown than at the invert; or the hydraulic head is uniform and its value is h_a (uniform head BC to calculate *Q2*; type II). In models representing tunnels type IIIb, a 3rd-kind (transfer, Cauchy type) BC is set at this boundary. The 3rd-kind BC accounts for a lining without the need of discretizing the lining. Instead, finite elements bordering the tunnel perimeter need to be assigned an outflow transfer rate c_t reducing tunnel inflow. This transfer rate c_t is given by the ratio of the hydraulic conductivity k_l and the thickness d of the resisting layer at the boundary (Diersch, 2009), which in our case is the lining:

$$c_t = k_l/d. \qquad (5)$$

The normal flux q through the resisting layer is approximated by the Darcy equation (Diersch, 2009)

$$q = c_t\,(h_{aq} - h_a) \qquad (6)$$

where $(h_{aq} - h_a)$ is the difference of the calculated hydraulic head in the aquifer at the tunnel perimeter and the hydraulic head set as BC at the tunnel perimeter. Flow Q into the tunnel is then calculated by the fluid mass exiting the model domain (Diersch, 2009):

$$Q = \int q \; dF \qquad (7)$$

where F is the Area on the tunnel perimeter given by the length times the depth of the considered section of the tunnel boundary (in our 2D models the calculated inflow assumes a thickness in the third dimension of 1 m, i.e., the flow rates are given per tunnel meter) (Figure 5).

[Figure 5 near here]

5. Analytical versus numerical solutions

The analytical solutions are based on a situation where the hydraulic head at the aquifer boundary above the tunnel is uniform. The groundwater table above the tunnel is not drawn down by the drainage effect of the tunnel, because the groundwater drawdown is balanced by groundwater recharge. This condition is also realized in the numerical models by setting a uniform head BC at this boundary. However, the drainage effect of the tunnel decreases the hydraulic head in the surroundings of the tunnel. While the analytical solutions assume a semi-infinite aquifer, the extent of the (spatially distributed) numerical models is finite. The decrease in hydraulic head due to the tunnel drainage cannot be accounted for at these boundaries, because a specified head or a no-flow boundary is set at these boundaries. If the outer model boundaries at the sides and below the tunnel are close to the tunnel (where the drainage effect of the tunnel is significant), it can be expected that numerical models using a specified head BC overestimate tunnel inflow, because the hydraulic head assigned to these boundaries is too high. If a no-flow BC is set at the lateral and bottom boundaries, it can be expected that numerical models underestimate tunnel inflow, because these boundaries cannot contribute to flow. The larger the model extent, the closer the numerical solution will approximate the analytical solution, because the drainage effect of the tunnel gets increasingly smaller when moving away from the tunnel.

Figure 6 shows the difference between analytically and numerically calculated tunnel inflows for type I tunnels (*Q1*) and type II tunnels (*Q2*) depending on the extent *ME* of the model domain (c.f., Figure 4). In this Figure, tunnel inflows are normalized to the analytical solution (i.e., the numerical solution is divided by the analytical solution, and the analytical solution equals 1). The numerical simulations used either a specified head or a no-flow BC at the lateral and bottom boundaries. If *ME* is only 10 times the tunnel radius *r* (e.g., *r* = 5 m and *ME* = 50 m; this corresponds to the geometrical setup shown in Figure 3), the numerical solution overestimates the (exact) analytical solution by more than 25 % if specified head BC are used, and underestimates the analytical solution by approximately 30 % if no-flow BC are used. Considering that the model extent shown in Figure 3 is rather typical if focus is placed on flow processes at the tunnel perimeter, the error of the numerical solution is large. If we consider an error smaller than 10 % to be acceptable for practical purposes, the extent of the model domain must be at least 20 times the tunnel radius (Figure 6).

[Figure 6 near here]

The calculations illustrated in Figure 6 are valid for unlined tunnels (type I), where inflow is not reduced by a lining, and for lined tunnels with drainage layer (type II). However, the drainage effect of a tunnel will be strongly reduced if the tunnel is lined and lacks a drainage layer (type III tunnels). The effect of a lining surrounding a tunnel without drainage layer on the accuracy of the numerical solution is shown in Figures 7 and 8. We calculated tunnel inflow *Q1* (uniform head BC at the tunnel perimeter) using discretized linings (type IIIa) with different hydraulic conductivity k_l and thickness *d*. We normalized the solution of models with different model extents *ME* to the solution of the model with *ME*/*r* = 200. This normalization is based on the fact that the solution of the model with *ME*/*r* = 200 is close to the analytical solution, as was shown above (c.f., Figure 6) (we cannot normalize it to the analytical solution, because analytical solutions accounting for type III tunnels do not exist). Just as in the above described cases of tunnels without a lining or with a drainage layer behind the lining (c.f., Figure 6), the accuracy of calculated tunnel inflows decreases if the extend of the model domain decreases. However, the accuracy also depends on the lining's resistance to flow, given by the hydraulic conductivity k_l (expresses by the ratio k_l/k_{aq}) and the thickness d of the lining (expressed by the ratio d/r). If the hydraulic conductivity of the lining is two orders of magnitude lower than that of the aquifer (k_l/k_{aq} < 1E-2) and the thickness of the tunnel lining is 0.1 times the tunnel radius (e.g., d=0.5 m and r=5 m), the deviation of inflow calculated with the model having the smallest model extent (ME/r = 10) from inflow calculated with the model having the largest model extent (ME/r = 200) is approximately 5 % (Figure 7). If the thickness of the tunnel lining is as small as 0.02 times the tunnel radius (e.g., d=0.1 m and r=5 m) and the ratio k_l/k_{aq} is 1E-6 (e.g., k_l=1E-10 m/s and k_{aq}=1E-4 m/s), inflow calculated with the model having the smallest model extent (ME/r = 10) is almost the same as inflow calculated with the model having the largest model extent (ME/r = 200) (Figure 8, solid lines). However, if the ratio k_l/k_{aq} is as mall as 1E-2 (e.g., k_l=1E-10 m/s and k_{aq}=1E-8 m/s), inflows calculated with the model having the smallest model extent (ME/r = 10) are up to 25 % higher than those calculated with the model having the largest model extent (ME/r = 200), depending on the thickness of the lining (Figure 8, dashed lines). From this it follows that a relatively small model extent is only sufficient to calculate tunnel inflow for practical purposes if the tunnel is lined and lacks a drainage layer and, at the same time, if the hydraulic conductivity of the lining is several orders of magnitude lower than the conductivity of the aquifer ($k_l/k_{aq} \leq$ ~1E-6) or if the lining is thick ($d/r \geq$ ~0.1). In highly permeable aquifers (k_{aq}= 1E-4 m/s), for example, a relatively small model is sufficient also for thin liners. In other aquifers (e.g., k_{aq}= 1E-8 m/s), a large model extent (larger ~50 tunnel radii) is required to obtain accurate model results, unless the lining is thick.

[Figures 7 and 8 near here]

6. Unlined tunnels (*Q1*) versus lined tunnels with a drainage layer (*Q2*)

In this section, hydraulic differences between unlined tunnels (type I) and lined tunnels having a drainage layer (type II) are discussed. Figure 9 shows calculated tunnel inflows using the analytical solutions for *Q1* (elevation head BC at tunnel perimeter) and *Q2* (uniform head BC) (c.f., chapter 3). Tunnel inflows are calculated depending on the depth of the tunnel under the groundwater table (upper aquifer boundary) relative to the tunnel radius (relative depth of tunnel $(h+H)/r$; H=0 m in all calculations). In this figure, inflows are normalized to *Q1*, i.e., the analytical solution for *Q2* is divided by the analytical solution for *Q1*, and the solution for *Q1* equals 1. The hydraulic head in the drainage layer h_a to calculate *Q2* is either set at $h - r$ (i.e., the drainage level corresponds to the level of the tunnel invert), at h (i.e., the drainage level corresponds to the level of the tunnel center), or at $h + r$ (i.e., the drainage level corresponds to the level of the tunnel crown). Tunnel inflows *Q2* are higher than inflows *Q1* if the head in the drainage layer corresponds to the level of the invert or the center (i.e., the outlet of the drainage layer is at the level of the invert or center). Tunnel inflows *Q2* are lower than inflows *Q1* if the head in drainage layer corresponds to the level of the crown (i.e., the outlet of the drainage layer is at the level of the crown). Differences between *Q1* and *Q2* become small in deep tunnels, i.e., if the tunnel is located deeper than 10 tunnel radii under the groundwater table ($(h+H)/r$ > 10). If the head in the drainage layer corresponds to the level of the tunnel center, *Q1* and *Q2* are almost equal in deep tunnels. In shallow tunnels (e.g., $(h+H)/r$ < 5), differences between *Q1* and *Q2* are large. For example, if the crown of a tunnel with 5 m radius is located only 1 m under the groundwater table ($(h+H)/r$ = 1.2; corresponds to the first dot from left in the data series shown in Figure 9), tunnel inflow *Q2* is more than three times higher than *Q1* if the head in the drainage layer corresponds to the level of the tunnel invert. On the other hand, *Q2* is only about one third of *Q1* if the head in the drainage layer corresponds to the level of the tunnel crown. In engineering practice, differences between flow rates at the crown and the invert can become important. Butscher et al. (2011a), for example, calculated flow rates at certain positions around the tunnel to make predictions of the swelling potential of clay-sulfate rocks in tunneling.

[Figure 9 near here]

Numerical groundwater models can be used to calculate the spatial distribution of the hydraulic head field in the surroundings of the tunnel and differences in flow rates at the tunnel perimeter. Figure 10 shows differences in inflows at the upper and lower half of the tunnel perimeter depending on the depth of the tunnel under the groundwater table ($(h+H)/r$) for *Q1* and *Q2*. In this figure, tunnel inflows at the upper half are normalized to inflows at the lower half of the tunnel perimeter (i.e., inflow at the upper half is divided by the inflow at the lower half). For unlined (type I) tunnels with an elevation head BC at the tunnel perimeter, inflow *Q1* at the upper half (or crown) is lower than at the lower half (or invert) (explanation will follow). For lined tunnels with a drainage layer (type II tunnels) and a uniform head BC at the tunnel perimeter corresponding to tunnel center ($h_a = h$), inflow *Q2* at the upper half is higher than at the lower half. Differences in inflow between the upper and lower half decrease if the depth of the tunnel under the groundwater table increases, and the differences are more pronounced for type II tunnels (*Q2*).

[Figure 10 near here]

The difference in inflows between type I and type II tunnels as well as the differences in inflows at the upper and lower half of the tunnel perimeter, can be explained if we look at Figure 11. This figure shows the spatial distribution of the hydraulic head calculated for an unlined (type I) tunnel using the elevation head BC (*Q1*, Figure 11 a)) and for a lined tunnel with drainage layer (type II) using the uniform head BC (*Q2*, Figure 11 b)). In the shown example, the relative depth of the tunnel under the groundwater table is 4 tunnel radii ($(h+H)/r$=4), and the head in the drainage layer corresponds to level of the tunnel center (h_a=h). In the case of a lined tunnel with drainage layer (type II), the hydraulic gradients are higher at the crown than at the invert, explaining the higher inflow *Q2* at the crown (c.f., Figure 10). The gradients at the crown are higher because the difference between the head at the groundwater table and at the tunnel perimeter has to be accommodated within a limited space above the tunnel, while the same difference in hydraulic head is accommodated in the (theoretically) semi-infinite aquifer under the tunnel (Figure 11b)). This effect holds also for unlined (type I) tunnels, but it is additionally affected by the influence of the elevation head BC at the tunnel perimeter, where the hydraulic head is lower at the invert than at the crown (Figure 11 a)). The lower head at the invert than at the crown causes the gradient of the head (head differences) to be higher at the invert than at the crown. Hence, inflows are higher at the invert than at the crown in unlined tunnels. The uniform head BC at the perimeter of lined tunnels with a drainage layer (type II) is expressed by the concentric array of the head contour lines around the tunnel (Figure 11 b)). The elevation head BC with decreasing head from the crown to the invert leads to counter lines of the hydraulic head that intersect the tunnel perimeter (Figure 11 a)). According to the hydraulic head field around the tunnel, groundwater flow near the tunnel is radial towards lined tunnels with a drainage layer (type II), but is inclined with a downward directed component towards unlined tunnels (type I).

[Figure 11 near here]

7. 1st-kind BC with discretized lining versus 3rd-kind BC without discretizing the lining at tunnel perimeter

In this section, we compare inflows into lined tunnels without drainage layer using a 1st-kind BC (specified head, Dirichlet type) with inflows using a 3rd-kind BC (transfer rate, Cauchy type) at the tunnel perimeter. Using a 1-st-kind BC requires discretizing the lining and specifying a hydraulic conductivity k_l and thickness d of the lining. Using a 3rd-kind BC eliminates the need to discretize the lining, but requires specifying an outflow transfer rate c_t for elements bordering the tunnel perimeter in order to account for limited tunnel inflow due to the lining. The former approach corresponds to type IIIa in Table 1; the latter corresponds to type IIIb.

Figure 12 compares calculated tunnels inflows $Q1$ calculated with a 1st-kind BC at the tunnel perimeter and a discretized lining with inflows $Q1$ calculated with a 3rd-kind BC at the tunnel perimeter without discretizing the lining. In this figure, $Q1$ calculated with a 3rd-kind BC is normalized to $Q1$ calculated with a 1st-kind BC. $Q1$ is shown in relation to the relative hydraulic conductivity k_l/k_{aq} of the lining for different relative thicknesses d/r of the lining. The transfer rate c_t is given by $c_t = k_l/d$ (c.f., equation (5)). The figure shows that differences between calculated inflows using a 1st-kind and 3rd-kind BC are nearly independent of the hydraulic conductivity of the lining. Differences become slightly smaller if k_l approaches k_{aq}. However, the differences strongly increase with increasing lining thickness. Inflow calculated with a 3rd-kind BC at the tunnel perimeter without discretizing the lining is generally lower than inflow calculated with a 1st-kind BC and a discretized lining. For example, if the thickness of the lining is 0.2 tunnel radii (e.g., d=1 m and r=5 m), $Q1$ calculated with a 3rd-kind BC at the tunnel perimeter is about 9 % lower than $Q1$ calculated with a 1st-kind BC. When using a 3rd-kind BC at the tunnel perimeter without discretizing the lining, the normal flux q through the lining is approximated by the Darcy equation assuming a constant hydraulic gradient normal to the lining in the aquifer at the position of the (non-discretized) lining (c.f., equation (6)). This approximation leads to inaccurate results if the lining is thick, as shown in Figure 12.

Discretizing the tunnel lining is often cumbersome in finite element models, because the thickness of the lining is typically very low compared to the extent of the model. If one assumes that an error in calculated inflow of 10 % is acceptable for practical purposes, the use of a 3rd-kind BC is helpful in many cases. It allows one to dispense with discretizing the lining if the thickness of the lining is less than 0.2 tunnel radii (e.g., less than 1 m lining around a tunnel with a radius of 5 m), which is rather typical in tunneling.

[Figure 12 near here]

8. Conclusions

The study highlights the effects of different types of tunnel support structures on tunnel inflow. The presented comparison of analytical solutions with numerical models suggests that numerical models provide estimates of tunnel inflows with sufficient accuracy for practical purposes only if the tunnel is lined and has no drainage layer surrounding the lining and, at the same time, if the hydraulic conductivity of the lining is several orders of magnitude higher than the hydraulic conductivity of the aquifer, or if the lining is thick. If the tunnel is unlined or has a drainage layer surrounding the lining, the extent of the model domain must be large with respect to the extent of the tunnel to provide accurate results. It was shown that inflows are higher for a lined tunnel with drainage layer than for an unlined tunnel, if the head in the drainage layer corresponds to the level of the tunnel center or invert. If the head in the drainage layer corresponds to the level of the tunnel crown, inflows are higher for an unlined tunnel. The differences become smaller if the depth of the tunnel under the groundwater table increases. An advantage of numerical models over analytical solutions is that only the former can be used to calculate different inflow rates at different positions of the tunnel perimeter. For unlined tunnels (elevation head BC), inflows are higher at the invert than at the crown. For lined tunnels with drainage layer (uniform head BC), the reverse is true. The differences between inflows at the crown and invert decrease with increasing depth of the tunnel under the groundwater table. The numerical solution for flow into lined tunnels without drainage layer using a 3rd-kind BC, without discretizing the lining, underestimates inflows using a 1st-kind BC and a discretized lining. Using a 3rd-kind BC is especially inaccurate if the lining is thick compared to the tunnel radius. Nevertheless, the approach using a 3rd-kind BC is useful because it renders sufficiently accurate results in many practical situations while being simpler.

Acknowledgements

The author wants to thank Herbert H. Einstein for constructive discussion and Antonio Bobet for valuable comments on the manuscript. This research was funded by a grant of the Swiss National Science Foundation (SNF grant no. PBBSP2-130955).

References

Bear, J., 1972. Dynamics of fluids in porous media. American Elsevier, New York.

Butscher, C., Huggenberger, P., Zechner, E., Einstein, H.H., 2011a. Relation between hydrogeological setting and swelling potential of clay-sulfate rocks in tunneling. Eng. Geol. 122 (2–4), 204–214.

Butscher, C., Einstein, H.H., Huggenberger, P., 2011b. Effects of tunneling on groundwater flow and swelling of clay-sulfate rocks. Water Resour. Res. 47, W11520.

Diersch, H.-J.G., 2009. FEFLOW - Finite Element Subsurface Flow & Transport Simulation System, Reference Manual, DHI-WASY GmbH, Berlin, Germany.

El Tani, M., 2003. Circular tunnel in a semi-infinite aquifer. Tunn. Undergr. Space Technol. 18 (1), 49–55.

El Tani, M., 2010. Helmholtz evolution of a semi-infinite aquifer drained by a circular tunnel. Tunn. Undergr. Space Technol. 25, 54–62.

Fernández, G., Alvarez, T. A., 1994. Seepage-induced effective stresses and water pressures around pressure tunnels. J. Geotech. Eng. 120 (1), 108–128.

Font-Capo, J., Vázquez-Suñé, E., Carrera, J., Martí, D., Carbonell, R., Pérez-Estaun, A., 2011. Groundwater inflow prediction in urban tunneling with a tunnel boring machine (TBM). Eng. Geol. 121 (1–2), 46–54.

Jacob, C.E., Lohman, S.W., 1952. Nonsteady flow to a well of constant drawdown in an extensive aquifer. Trans. Am. Geophys. Union 33 (4), 559–569.

Kolymbas, D., Wagner, P., 2007. Groundwater ingress to tunnels – the exact analytical solution. Tunn. Undergr. Space Technol. 22 (1), 23–27.

Lei, S., 1999. An analytical solution for steady flow into a tunnel. Ground Water 37, 23–26.

Maréchal, J.-C., Perrochet P., 2003. Nouvelle solution analytique pour l'étude de l'interaction hydraulique entre les tunnels alpins et les eaux souterraines. Bull. Soc. Géol. Fr. 174 (5), 441–448.

Park, K.-H., Owatsiriwong, A., Lee, J.-G., 2008. Analytical solution for steady-state groundwater inflow into a drained circular tunnel in a semi-infinite aquifer: A revisit. Tunn. Undergr. Space Technol. 23 (2), 206–209.

Perrochet, P., 2005a. Confined flow into a tunnel during progressive drilling: An analytical solution. Ground Water 43 (6), 943–946.

Perrochet, P., 2005b. A simple solution to tunnel or well discharge under constant drawdown. Hydrogeol. J. 13, 886–888.

Perrochet, P., Dematteis, A., 2007. Modeling transient discharge into a tunnel drilled in a heterogeneous formation. Ground Water 45 (6), 786–790.

Yang, S.-Y., Yeh, H.D., 2007. A closed-form solution for a confined flow into a tunnel during progressive drilling in a multi-layer groundwater flow system. Geophys. Res. Lett. 34, L07405.

Tables

Table 1: Overview of types of tunnel support structure, boundary conditions at tunnel perimeter and representation of lining. In numerical models, discretization of the tunnel lining (type IIIa tunnels) involves specifying the hydraulic properties of the lining for the finite elements at the lining's position. The drainage layer and impermeable lining of type II tunnels do not have to be discretized.

Type I: **Unlined tunnel**	**Type II:** **Lined tunnel with drainage layer**	**Type IIIa:** **Lined tunnel without drainage layer**	**Type IIIb:** **Lined tunnel without drainage layer**
	Drainage layer		
No	Yes	No	No
	Lining		
No	Yes (impermeable)	Yes (discretized)	Yes (not discretized)
	Type of BC		
1^{st}-kind (Dirichlet), Elevation head BC	1^{st}-kind (Dirichlet), Uniform head BC	1^{st}-kind (Dirichlet), Elevation head BC	3^{rd}-kind (Cauchy), Elevation head BC
	Head at tunnel perimeter		
y	h_a (c.f., Figure 1)	y	y
	Variables characterizing lining		
-	-	Hydraulic conductivity k_l, Thickness d	Outflow transfer rate c_t
	Flow into tunnel		
Q1	*Q2*	*Q1*	*Q1*

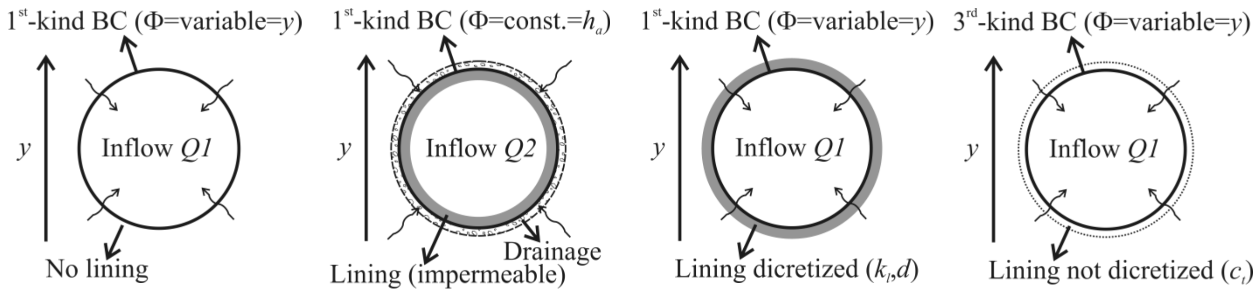

NOTICE: this is the author's version of a work that was accepted for publication in Tunnelling and Underground Space Technology. Changes resulting from the publishing process, such as peer review, editing, corrections, structural formatting, and other quality control mechanisms may not be reflected in this document. Changes may have been made to this work since it was submitted for publication. A definitive version was subsequently published in TUNNELLING AND UNDERGROUND SPACE TECHNOLOGY 32, 158-167, (2012), DOI: 10.1016/j.tust.2012.06.007

Table 2: Notation of variables and, if not stated differently in the text, values of parameters used in this study.

Variable	Description (unit)	see Figure(s)	Value
c_t	Transfer rate (1/s)	5	1E-10
d	Thickness of tunnel lining (m)	3	0.5
F	Area on tunnel perimeter (m^2)	5	-
h	Depth of tunnel center (m)	2, 4	50
H	Groundwater level (m)	2	0
h_a	Uniform hydraulic head at tunnel perimeter (m)	1	-50
h_{aq}	Hydraulic head in aquifer at tunnel perimeter (m)	3, 5	-
k_{aq}	Hydraulic conductivity of aquifer (m/s)	3	1E-4
k_l	Hydraulic conductivity of tunnel lining (m/s)	3	1E-10
ME	Model extent (left, right and down from tunnel center) (m)	4	50
q	Groundwater flux (m/s)	5	-
Q	Groundwater flow (volumetric flow rate) (m^3/s)	5	-
$Q1$	Tunnel inflow calculated for elevation head BC (m^3/s)	-	-
$Q2$	Tunnel inflow calculated for uniform head BC (m^3/s)	-	-
r	Tunnel radius (m)	2, 3	5
x	Horizontal axis (m)	2, 3	-
y	Vertical axis (elevation) (m) (Reference datum: $y = 0$)	2, 3	-
Φ	Hydraulic (total) head (m)	2, 3	-

NOTICE: this is the author's version of a work that was accepted for publication in Tunnelling and Underground Space Technology. Changes resulting from the publishing process, such as peer review, editing, corrections, structural formatting, and other quality control mechanisms may not be reflected in this document. Changes may have been made to this work since it was submitted for publication. A definitive version was subsequently published in TUNNELLING AND UNDERGROUND SPACE TECHNOLOGY 32, 158-167, (2012), DOI: 10.1016/j.tust.2012.06.007

Figures

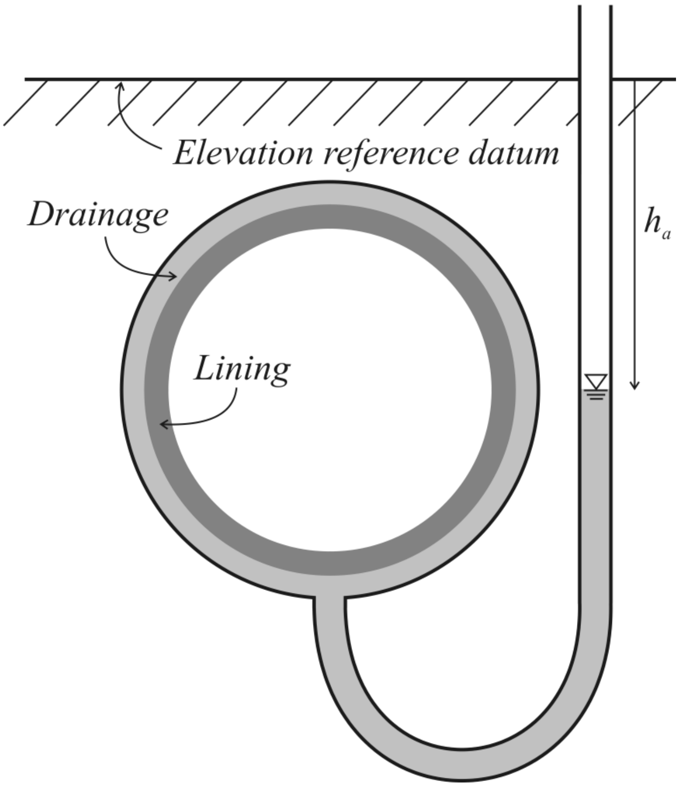

Figure 1: Drained tunnel with uniform hydraulic head h_a at tunnel perimeter.

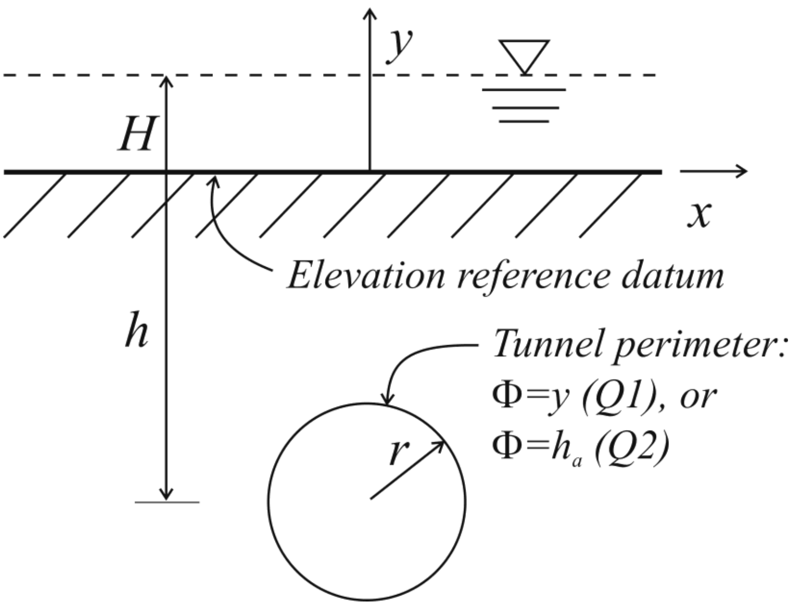

Figure 2: Circular tunnel in a semi-infinite aquifer (from: Park et al., 2008). Variables: see Table 2.

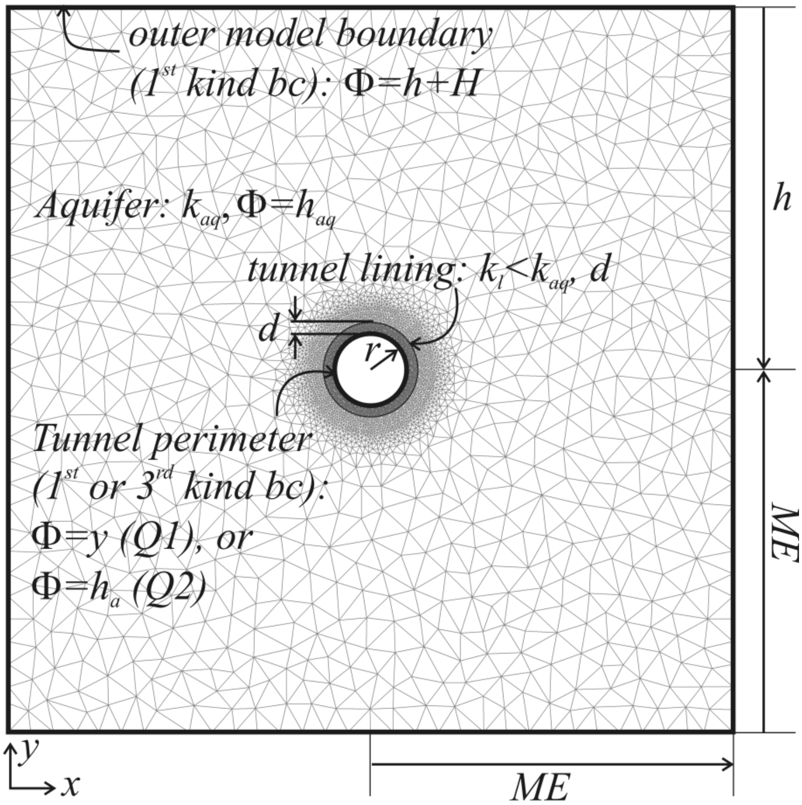

Figure 3: Finite element groundwater model with circular tunnel. Variables: see Table 2; h_a: also see Figure 1.

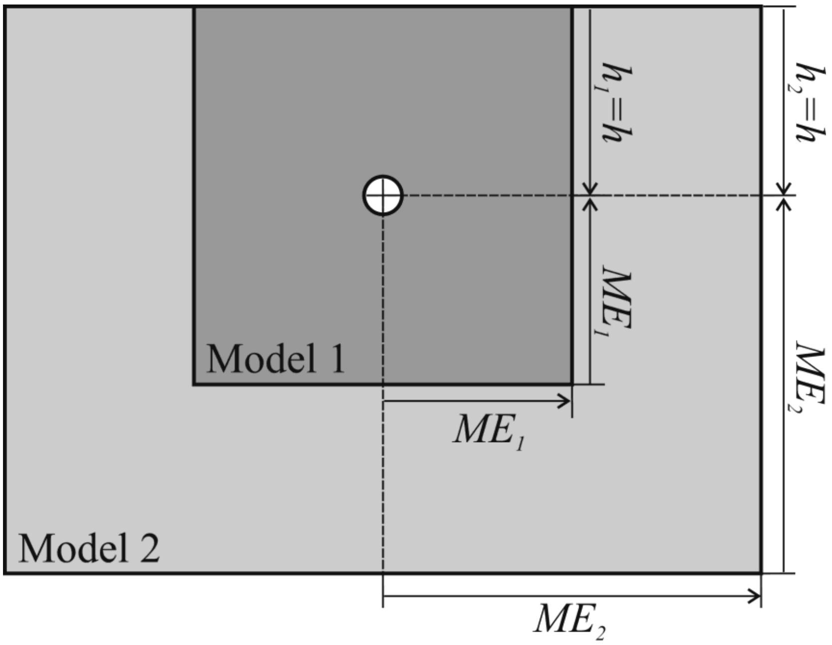

Figure 4: Depth of tunnel h and extent of model domain ME for two models with different ME. Subscripts refer to model 1 and 2.

NOTICE: this is the author's version of a work that was accepted for publication in Tunnelling and Underground Space Technology. Changes resulting from the publishing process, such as peer review, editing, corrections, structural formatting, and other quality control mechanisms may not be reflected in this document. Changes may have been made to this work since it was submitted for publication. A definitive version was subsequently published in TUNNELLING AND UNDERGROUND SPACE TECHNOLOGY 32, 158-167, (2012), DOI: 10.1016/j.tust.2012.06.007

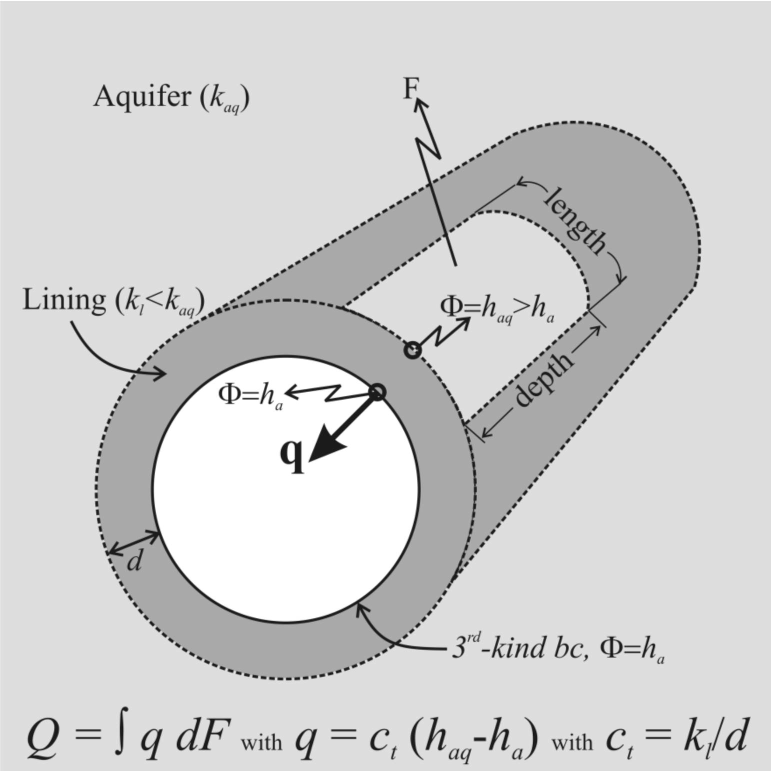

Figure 5: Calculation of tunnel inflow Q using a 3rd-kind BC, which includes specifying the hydraulic head (here: h_a; c.f., Figure 1) and an outflow transfer rate c_t at the tunnel perimeter. Variables: see Table 2.

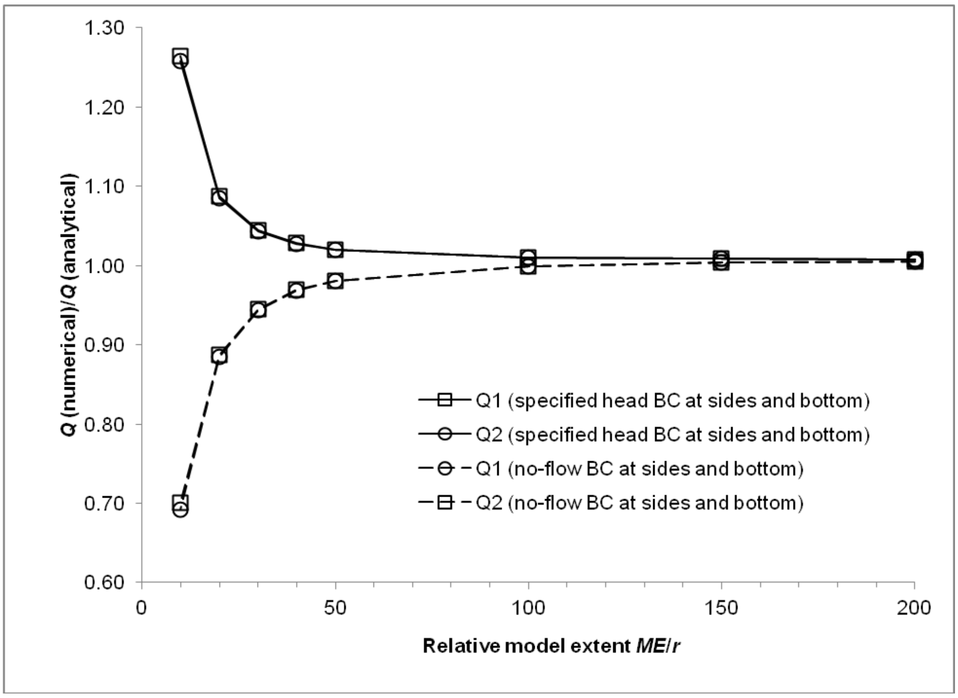

Figure 6: Difference between numerically and analytically calculated inflows into unlined tunnels (type I tunnels, *Q1*) and into the drainage layer of lined tunnels (type II tunnels, *Q2*) plotted against extent of model domain. Shown are numerical solutions *Q1* and *Q2* normalized to the analytical solutions (analytical solutions equal 1). At the lateral and bottom boundaries, either specified head BC (solid lines) or no-flow BC (dashed lines) are used in the numerical models.

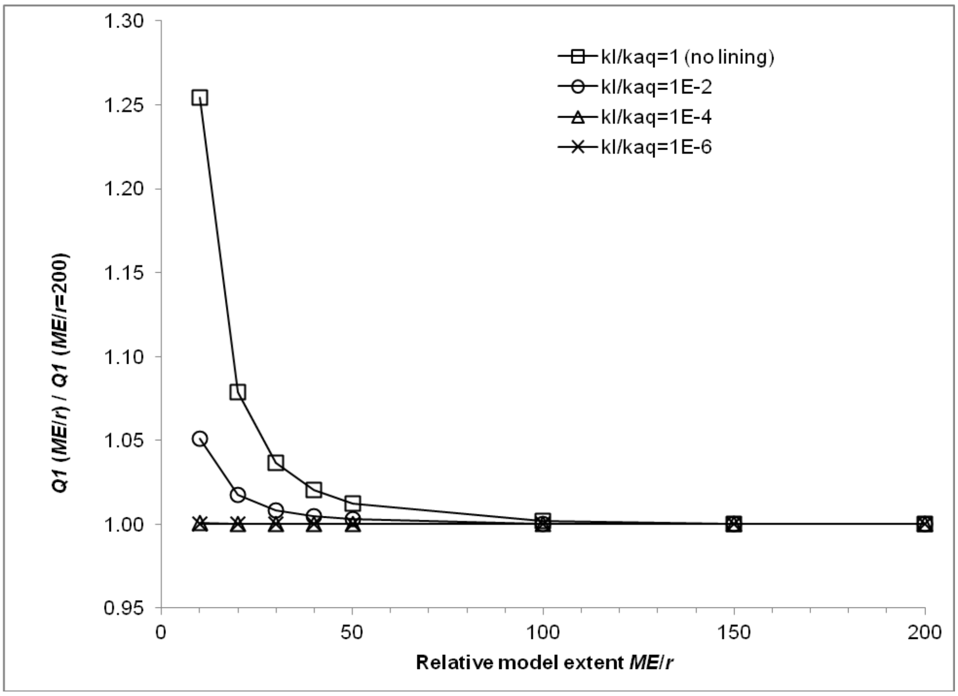

Figure 7: Inflow into lined tunnels without drainage layer (type IIIa tunnels) calculated for different hydraulic conductivities k_l of the lining (expressed by the ration k_l/k_{aq}), plotted against extent of model domain. The thickness *d* of the lining is 0.1*r* (tunnel radii). Shown are numerical solutions *Q1* normalized to the numerical solution with a relative model extent *ME*/*r* = 200 (solution with a relative model extent *ME*/*r* = 200 equals 1; this solution deviates little from the analytical solution (c.f., Figure 6), which is not available for type III tunnels).

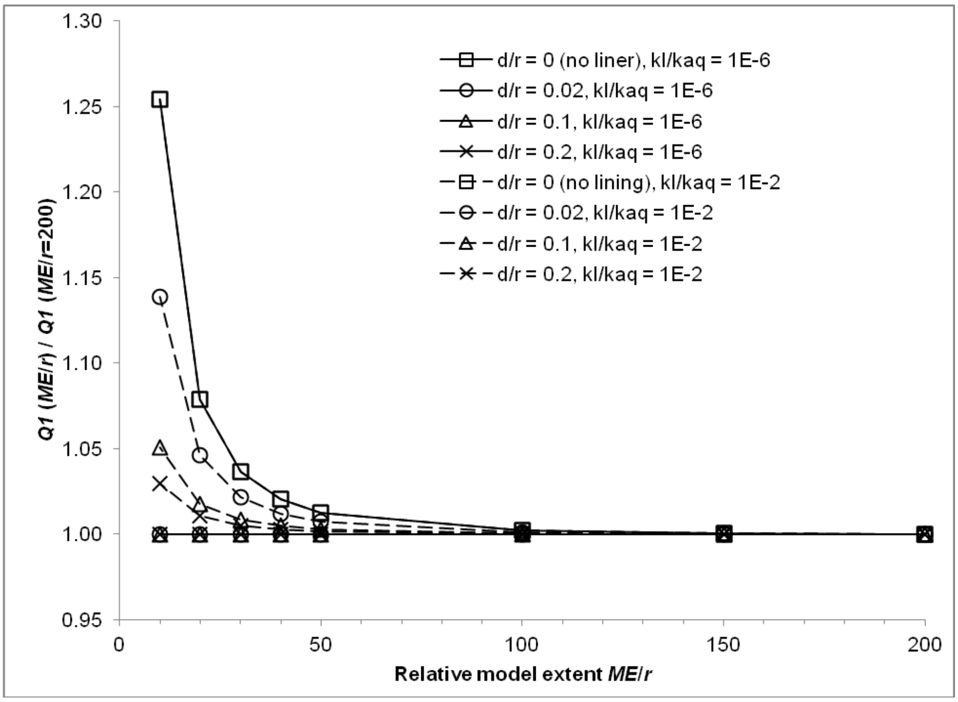

Figure 8: Inflow into lined tunnels without drainage layer (type IIIa tunnels) calculated for different thicknesses *d* (expressed by the ration *d*/*r*), plotted against extent of model domain. The relative hydraulic conductivity k_l of the linings is 1E-6k_{aq} (solid lines) or 1E-2k_{aq} (dashed lines). Shown are numerical solutions *Q1* normalized to the numerical solution with a relative model extent *ME*/*r* = 200 (solution with a relative model extent *ME*/*r* = 200 equals 1; this solution deviates little from the analytical solution (c.f., Figure 6), which is not available for type III tunnels).

NOTICE: this is the author's version of a work that was accepted for publication in Tunnelling and Underground Space Technology. Changes resulting from the publishing process, such as peer review, editing, corrections, structural formatting, and other quality control mechanisms may not be reflected in this document. Changes may have been made to this work since it was submitted for publication. A definitive version was subsequently published in TUNNELLING AND UNDERGROUND SPACE TECHNOLOGY 32, 158-167, (2012), DOI: 10.1016/j.tust.2012.06.007

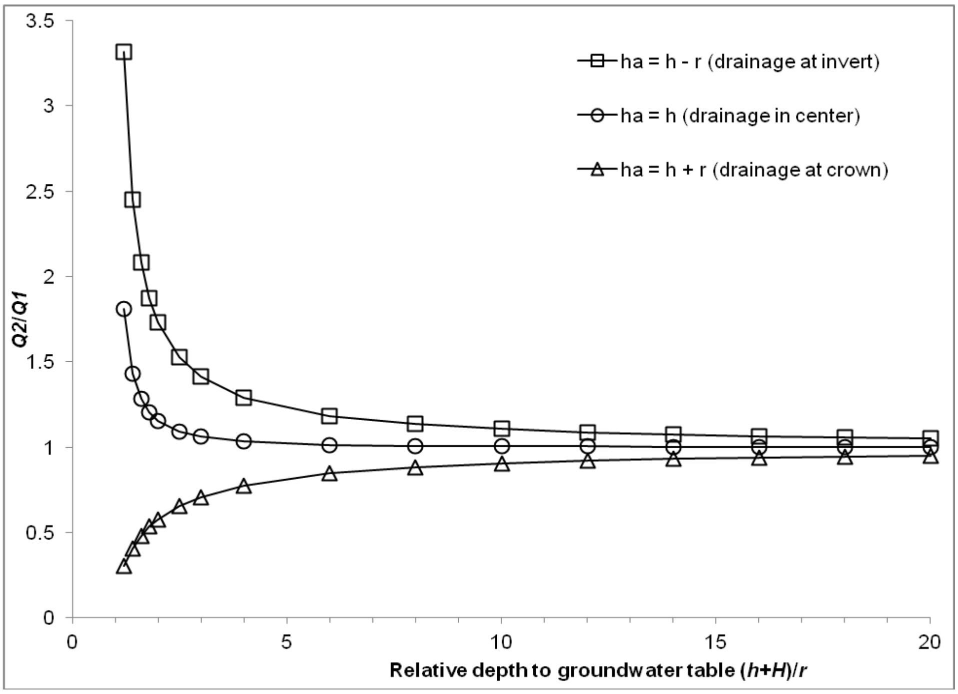

Figure 9: Difference between inflow *Q1* into unlined tunnels (type I) using an elevation head BC and inflow *Q2* into lined tunnels with drainage layer (type II) using a uniform head BC plotted against the relative depth of the tunnel under the groundwater table (analytical solutions; normalized to *Q1*). Shown are solutions for different hydraulic heads h_a in the drainage layer of type II tunnels to calculate *Q2*.

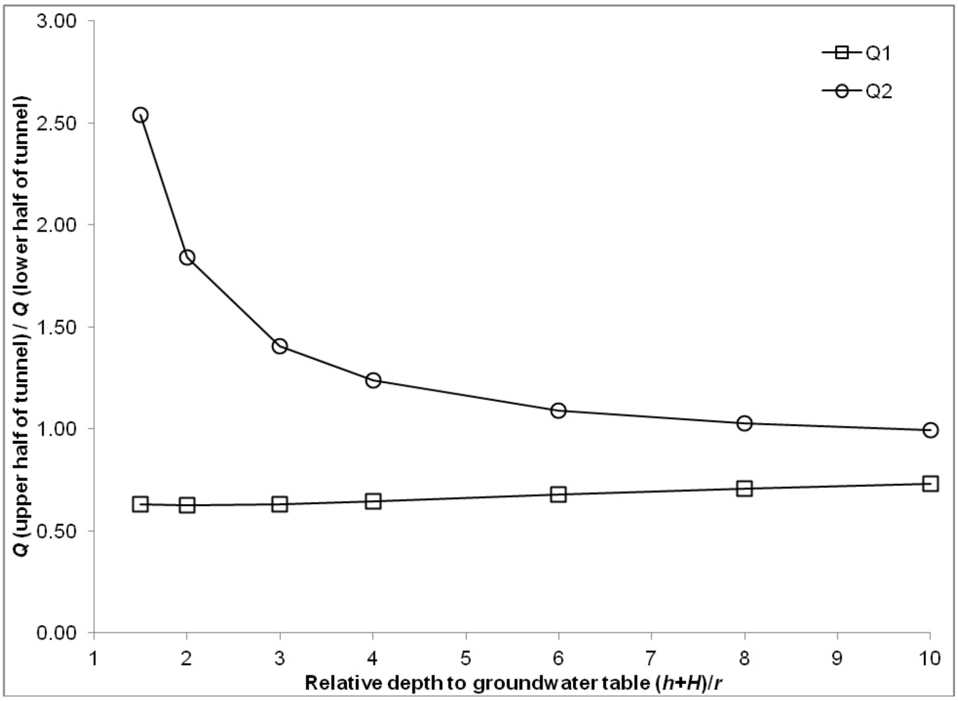

Figure 10: Inflow at upper half relative to the inflow at lower half of tunnel perimeter calculated for an unlined tunnel (type I) using an elevation head BC (*Q1*) and for a lined tunnel with drainage layer (type II) using a uniform head BC (*Q2* with $h_a = h$), plotted against the relative depth of the tunnel under the groundwater table.

NOTICE: this is the author's version of a work that was accepted for publication in Tunnelling and Underground Space Technology. Changes resulting from the publishing process, such as peer review, editing, corrections, structural formatting, and other quality control mechanisms may not be reflected in this document. Changes may have been made to this work since it was submitted for publication. A definitive version was subsequently published in TUNNELLING AND UNDERGROUND SPACE TECHNOLOGY 32, 158-167, (2012), DOI: 10.1016/j.tust.2012.06.007

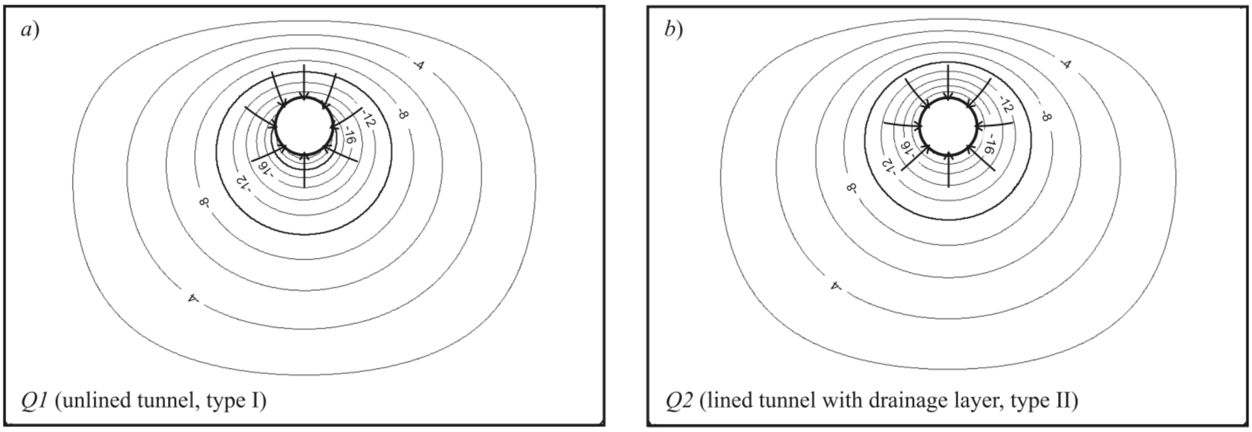

Figure 11: a) Distribution of hydraulic head in the aquifer and at the tunnel perimeter into an unlined tunnel (type I) using an elevation head BC (*Q1* with $h = 4r$); and b) into a lined tunnel with drainage layer (type II) using a uniform head BC (*Q2* with $h = 4r$ and $h_a = h$). $ME = 10r$. Arrows indicate groundwater flow direction. Variables: see Table 2.

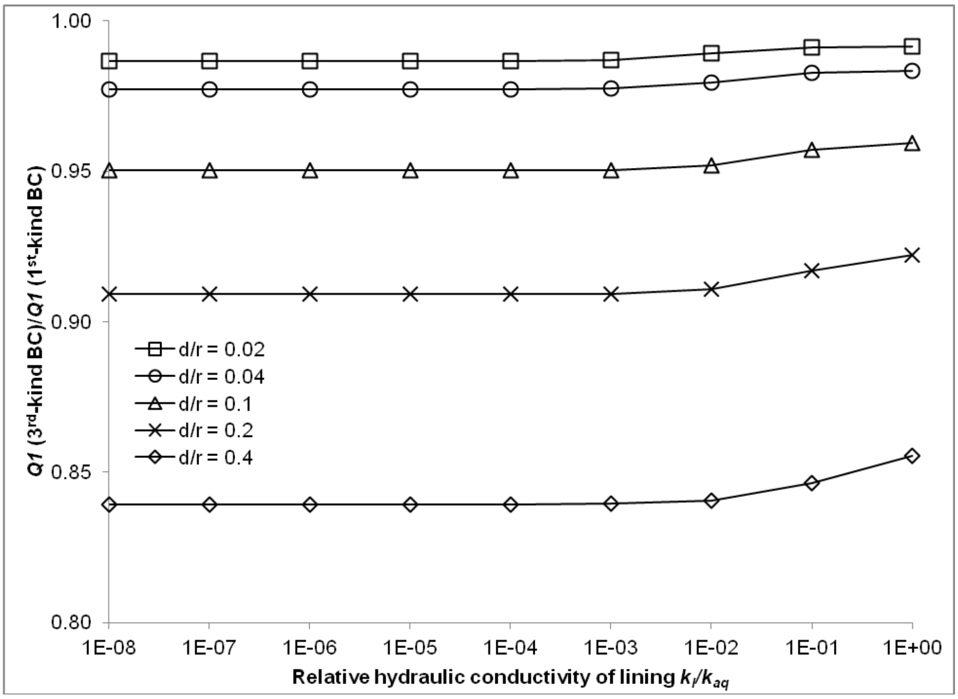

Figure 12: Difference between inflows *Q1* into lined tunnels without drainage layer calculated using a 1st-kind BC and a discretized lining (type IIIa) and using a 3rd-kind BC without discretizing the lining (type IIIb), plotted against the relative hydraulic conductivity of the lining (*Q1* using 3rd-kind BC normalized to *Q1* using 1st-kind BC). Different graphs represent different relative thicknesses of the lining.